Available online at www.sciencedirect.com
ScienceDirect
Journal of Power Sources 167 (2007) 491–498
JOURNAL OF POWER SOURCES
www.elsevier.com/locate/jpowsour

Polymer electrolytes based on an electrospun poly(vinylidene fluoride-*co*-hexafluoropropylene) membrane for lithium batteries

Xin Li [a], Gouri Cheruvally [a], Jae-Kwang Kim [a], Jae-Won Choi [a], Jou-Hyeon Ahn [a,*], Ki-Won Kim [b], Hyo-Jun Ahn [b]

[a] *Department of Chemical & Biological Engineering and ITRC for Energy Storage and Conversion, Gyeongsang National University, 900, Gajwa-dong, Jinju 660-701, Republic of Korea*
[b] *School of Nano and Advanced Materials Engineering and ITRC for Energy Storage and Conversion, Gyeongsang National University, 900, Gajwa-dong, Jinju 660-701, Republic of Korea*

Received 28 November 2006; accepted 10 February 2007
Available online 25 February 2007

Abstract

Electrospinning parameters are optimized for the preparation of fibrous membranes of poly(vinylidene fluoride-*co*-hexafluoropropylene) {P(VdF-HFP)} that consist of layers of uniform fibres of average diameter 1 μm. Electrospinning of a 16 wt.% solution of the polymer in acetone/*N*,*N*-dimethylacetamide (DMAc) (7/3, w/w) at an applied voltage of 18 kV results in obtaining membranes with uniform morphology. Polymer electrolytes (PEs) are prepared by activating the membrane with liquid electrolytes. The fully interconnected porous structure of the host polymer membrane enables high electrolyte uptake and ionic conductivities of 10^{-3} S cm^{-1} order at 20 °C. The PEs have electrochemical stability at potentials higher than 4.5 V versus Li/Li$^+$. A PE based on a membrane with 1 M $LiPF_6$ in ethylene carbonate (EC)/dimethyl carbonate (DMC), which exhibits a low and stable interfacial resistance on lithium metal, is evaluated for discharge capacity and cycle properties in Li/$LiFePO_4$ cells at room temperature and different current densities. A remarkably good performance with a high initial discharge capacity and low capacity fading on cycling is obtained.

Keywords: Electrospinning; Polymer electrolyte; Poly(vinylidene fluoride-*co*-hexafluoropropylene); Fibrous membrane; Lithium batteries

1. Introduction

Polymer electrolytes (PEs) have received considerable attention in recent years for application in rechargeable secondary batteries since they can offer systems that are lighter, safer and more flexible in shape compared with their liquid counterparts. In porous PEs, the polymer host in the form of a membrane with pores of nanometer to micrometer size is employed to retain the liquid electrolyte [1,2]. The membrane should have the capability to absorb the liquid electrolyte without leakage, be chemically compatible with electrode materials and adhere well to the electrode. Among the few polymers that meet these requirements, poly(vinylidene fluoride) (PVdF) and its copolymer, poly(vinylidene fluoride-*co*-hexafluoropropylene) {P(VdF-HFP)} have been found to be very promising as they have good electrochemical stability and affinity to electrolyte solutions [3]. Porous membranes of PVdF/P(VdF-HFP) are generally prepared by: (i) a solvent-casting method [4]; (ii) an extraction method, in which a plasticizer such as di-*n*-butyl phthalate (DBP) is extracted from a film constituting of the polymer and DBP [1,5]; or (iii) a phase inversion method using a solvent/non-solvent system [2,6–8]. In the modified Bellcore technology developed for the first practical polymer rechargeable battery in 1996, the extraction method was used to prepare the porous P(VdF-HFP) membrane [1]. Although these membranes possess good ionic conductivity and electrochemical stability, their capabilities at high-discharge rates are limited due to the nano-scale pore size and low porosity (∼50%) of the matrix. With the phase inversion method, microporous membranes (pore size: 0.1–1 μm) with >70% porosity can generally be obtained and can contain larger amounts of electrolyte solution. Increasing the pore size in the matrix from the nano- to

* Corresponding author. Tel.: +82 55 751 5388; fax: +82 55 753 1806.
E-mail address: jhahn@gsnu.ac.kr (J.-H. Ahn).

0378-7753/$ – see front matter © 2007 Elsevier B.V. All rights reserved.
doi:10.1016/j.jpowsour.2007.02.032

the micro-scale can help to enhance the mobility of ions and the ionic conductivity. Moreover, the resulting PEs show lower bulk impedance and higher rate capability [9].

Electrospinning is an alternative, simple and efficient way to prepare thin fibrous mats [10–12]. Interest in this mature technology was revived in the 1980s when it was demonstrated that the process could be used to fabricate ultrafine fibres and fibrous structures of various polymers with diameters down to submicrons or nanometers. In electrospinning, a high-voltage electric field is applied to a polymer fluid stream (solution or melt) that is delivered through a thin nozzle. This creates a charged jet. As the jet travels in air, the solvent evaporates to leave behind the fibre which gets deposited on a charged collector [10–12]. With proper control of the processing parameters, fibrous membranes with porosities of 30–90% and pore size in the range of sub-micrometers to a few micrometers can be made. The electrospun membranes find various applications in composite reinforcement, filtration systems, tissue templates, medical prosthesis, electromagnetic shielding and liquid crystal devices [11]. The electrospun membrane appears to be particularly suitable for use as a host matrix in microporous PEs because the fully interconnected pores with large surface area can function as efficient channels for ion conduction. The first report of such an application of the electrospun PVdF membrane for a lithium battery was published in 2003 by Choi et al. [13]. Subsequent studies in this area were focused on the suitability of electrospun membranes of PVdF [13–16], P(VdF-HFP) [17] and poly(acrylonitrile) (PAN) [18] for lithium-ion battery applications. A few patents have been filed on lithium secondary batteries that employ electrospun polymer membrane-based electrolytes [19]. By contrast, there have been no reports of the suitability of electrospun membrane-based PEs for lithium metal polymer batteries.

This study involves optimization of the process parameters for preparing a P(VdF-HFP) microfibrous membrane with a uniform morphology. The PEs are prepared by activation of the membrane with different liquid electrolytes and the electrochemical properties are evaluated. The suitability of the PEs based on electrospun membrane for room temperature lithium metal polymer batteries is also investigated.

2. Experimental

2.1. Preparation and characterization of electrospun membrane

The P(VdF-HFP) co-polymer (Kynar Flex 2801, $M_w = 4.77 \times 10^5$, VdF/HFP ratio: 88/12, Elf Atochem) was vacuum dried at 60 °C before use. The solvents, acetone and *N*,*N*-dimethylacetamide (DMAc) (HPLC grades, Aldrich), were used as received. Fibrous membranes were prepared by the typical electrospinning method at room temperature, as described in literature [10–12]. P(VdF-HFP) solutions of varying concentration (12–18 wt.%) were prepared in a mixed solvent of acetone/DMAc (in varying proportions, 3:7, 5:5 and 7:3, w/w) by mechanical stirring for 30 min at room temperature. The polymer solution was fed through a capillary using a syringe pump (KD Scientific, Model 210) and a high electric voltage (varied between 11 and 24 kV) was applied to the capillary by means of a power supply. A thin aluminum foil fixed on a grounded, stainless-steel current collector in the shape of a drum rotating at a specified speed was used to collect the charged polymer in the form of a membrane. The electrospun membrane was vacuum dried at 60 °C for 12 h before further use. The surface morphology of the membrane was observed with a scanning electron microscope (SEM-JEOL JSM 5600) and the average fibre diameter (AFD) was calculated based on micrographs taken at high magnifications. The porosity (P) was determined by the *n*-butanol uptake method, in which the dry membrane is immersed in *n*-butanol for 1 h, using the relation:

$$P\,(\%) = \frac{M_{\mathrm{BuOH}}/\rho_{\mathrm{BuOH}}}{(M_{\mathrm{BuOH}}/\rho_{\mathrm{BuOH}}) + (M_{\mathrm{m}}/\rho_{\mathrm{P}})} \times 100 \quad (1)$$

where M_m is the mass of the dry membrane, M_{BuOH} the mass of *n*-butanol absorbed and ρ_{BuOH} and ρ_P are the densities of *n*-butanol and polymer, respectively [17].

2.2. Preparation of PEs based on electrospun fibrous membrane

PEs were prepared by soaking the membrane for 1 h in liquid electrolyte solutions under an argon atmosphere in a glovebox ($H_2O < 10$ ppm). Four different electrolyte solutions were used: (i) 1 M lithium hexafluorophosphate ($LiPF_6$) in ethylene carbonate (EC)/dimethyl carbonate (DMC) (1:1, v/v); (ii) 1 M $LiPF_6$ in EC/diethyl carbonate (DEC) (1:1, v/v); (iii) 1 M lithium trifluoromethanesulfonate ($LiCF_3SO_3$) in propylene carbonate (PC); (iv) 1 M $LiCF_3SO_3$ in tetra(ethylene glycol) dimethyl ether (TEGDME). The lithium salts and organic solvents were supplied by Aldrich. $LiPF_6$ salt in mixed carbonate solvents was selected for the study because these electrolytes are generally employed in commercial lithium-ion batteries [20]. $LiCF_3SO_3$ was selected based on its high dissociation constant among the different lithium salts, which enables it to perform well even in comparatively low dielectric media like TEGDME [20].

2.3. Electrochemical measurements

Electrolyte uptake by the membrane was determined by soaking a circular piece of the membrane (diameter 1.5 cm) in each electrolyte solution. The weight of the wetted membrane was determined at different soaking intervals, taking care to remove the excess electrolyte remaining on the surface of the membrane by wiping softly with a tissue paper. The electrolyte uptake (ε) was calculated using the relation:

$$\varepsilon\,(\%) = \frac{M - M_0}{M_0} \times 100 \quad (2)$$

where M_0 is the mass of the dry membrane and M is the mass after soaking with electrolyte [14]. The ionic conductivities of the PEs, over the temperature range −20 to 80 °C, were measured by the AC impedance analysis using stainless-steel (SS) Swagelok cells with an IM6 frequency analyzer. The measurements were performed over the frequency range of 100 mHz to 2 MHz and at an amplitude of 10 mV. The interfacial resistance

(R_f) between the PE and lithium metal electrode was measured by the impedance response of Li/PE/Li cells over the frequency range 10 mHz to 2 MHz. The electrochemical stability was determined by linear sweep voltammetry (LSV) of Li/PE/SS cells at a scan rate of 1 mV s^{-1} over the range of 2–6 V at 25 °C.

The prototype lithium cell was fabricated by sandwiching the fibrous membrane based PE between a lithium metal anode (300 μm thickness, Cyprus Foote Mineral Co.) and lithium iron phosphate ($LiFePO_4$) cathode in SS Swagelok® type, circular cells of 23 mm diameter. The carbon-coated $LiFePO_4$ cathode active material was made in-house by mechanical activation followed by solid-state reaction at high temperature [21]. The charge–discharge and cycling tests were conducted in an automatic galvanostatic charge–discharge unit, WBCS3000 battery cycler (WonA Tech. Co.), between 2.5 and 4.0 V at room temperature. The experiments were run at different current density rates that ranged from 0.1 to 5 C.

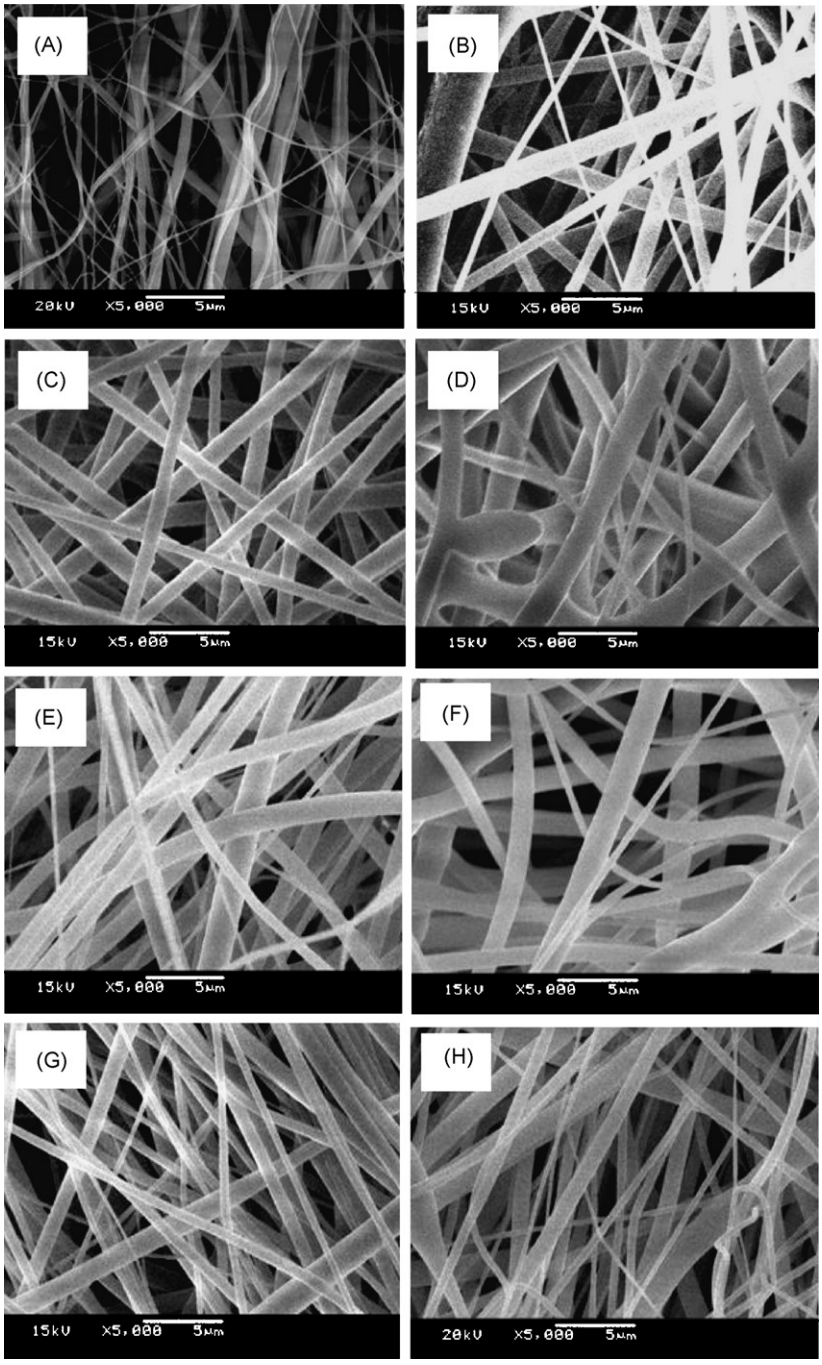

Fig. 1. Scanning electron micrographs of electrospun P(VdF-HFP) membranes under different processing conditions. (A–D) Effect of change in polymer concentration (wt.%): (A) 12, (B) 14, (C) 16 and (D) 18. Applied voltage: 18 kV, acetone:DMAc (7:3, w/w). (E and F) Effect of change in applied voltage (kV): (E) 11 and (F) 24. Polymer concentration: 16 wt.%, acetone/DMAc (7:3, w/w). (G and H) Effect of change in acetone:DMAc ratio (w/w): (G) 5:5 and (H) 3:7. Polymer concentration, 16 wt.%; applied voltage, 18 kV.

3. Results and discussion

3.1. Optimization of electrospinning process parameters

A number of parameters are known to influence the size and the morphology of the fibrous mat obtained by electrospinning process. These include: (i) system parameters such as the molecular weight, molecular weight distribution and architecture (linear, branched, etc.) of the polymer; (ii) solution properties such as viscosity, surface tension and conductivity; (iii) process parameters such as applied electric voltage, flow rate, concentration of solution, gap between the needle tip and collecting surface and motion of the target screen; (iv) ambient parameters such as temperature, humidity and air velocity of the chamber [11,12]. In the present study, some of the process parameters are optimized so as to obtain membranes that consist of bead-free fibres with uniform size and well-defined morphology. Based on a few preliminary experiments, the following process parameters have been optimized initially as: gap between spinneret and collector, 22 cm; spinneret needle size, 0.6 mm; solution feed rate, 0.1 mL min^{-1}; collecting drum rotation rate, 120 rpm.

The effect of varying polymer concentration, applied electric voltage and mixed solvent composition on the membrane morphology is shown in Fig. 1. The variations in processing conditions along with the fibre diameter range and AFD of the membranes obtained under these conditions are presented in Table 1. The SEM images (A–D) show the effect of change in concentration of the polymer solution between 12 and 18 wt.% in a mixture of acetone and DMAc (7:3, w/w), at 18 kV voltage. Polymer concentration is seen to influence strongly the fibre size as well as the size distribution. AFD increases with increasing polymer concentration. A similar increase in AFD with polymer concentration has been reported for an electrospun PVdF membrane [14,17]. Since the solution viscosity is proportional to the polymer concentration, higher solution viscosity leads to the deposition of fibres with larger diameters [11]. At lower polymer concentrations ($\leq$14 wt.%), a considerable amount of very thin fibres of 0.1–0.3 μm in diameter is observed. Uniform membrane morphology with a narrow range of fibre diameter and an AFD of 1 μm is obtained by electrospinning of a 16 wt.% solution.

The applied electric voltage also affects the membrane morphology to a considerable extent. Generally, a higher applied voltage ejects more fluid in a jet and thereby leads to a larger fibre diameter [11]. The morphologies obtained for the P(VdF-HFP) membranes with 16 wt.% solution in acetone:DMAc (7:3, w/w), processed under different voltages can be compared in Fig. 1C, E and F (18, 11 and 24 kV, respectively). 18 kV is found to be the optimum for obtaining the most uniform morphology, with a narrow distribution of fibre diameters. Application of a higher voltage of 24 kV results in the formation of a considerable portion of large fibres with a wider range of diameter. The change in acetone:DMAc weight ratio in the range 7:3, 5:5 and 3:7 (Fig. 1C, G and H, respectively) has lesser influence on the membrane morphology compared with polymer concentration and applied voltage. Uniform fibre morphology is obtained with a 7:3 ratio, i.e., with a slightly higher amount of acetone in the mixture. Based on these results, the optimum processing conditions were chosen to be 16 wt.% polymer solution in acetone:DMAc (7:3, w/w) and 18 kV applied voltage. The membrane thickness varies in the range 100–125 μm. The electrospun fibres are circular in cross-section with a smooth surface finish and the interlaying of the fibres generates the microporous structure with fully interconnected pores.

3.2. Electrolyte uptake of membrane

The fibrous membrane prepared under the optimized conditions was characterized for application as a host matrix for PEs. The porosity of the membrane as determined by *n*-butanol uptake is 59%, which is less compared with that reported (~75%) by Kim et al. [17] for membranes of AFD 1.3 μm. The difference might be due to the variations in experimental parameters adopted for electrospinning. It is inferred that the fibrous membrane in the present study contains more closely spaced fibres leading to decreased porosity. The electrolyte uptake of the membrane was determined in different electrolyte solutions over a period of 1 h and the results are shown in Fig. 2. The variation of electrolyte uptake is small with different electrolytes; it ranges from 165% for 1 M $LiPF_6$ in EC/DMC to 210% for 1 M $LiCF_3SO_3$ in TEGDME. The uptake process is very fast for all electrolytes and the maximum amount of liquid penetrates into the membrane within the initial few minutes. The fully interconnected pore structure of the membrane is beneficial in achieving this. Although TEGDME has a higher molecular size and viscosity compared with the other solvents (Table 2), the higher uptake observed for 1 M $LiCF_3SO_3$ in TEGDME electrolyte could be the result of better wetting and compatibility of the polymer with this solvent. An electrolyte uptake of ~330% with

Table 1
Morphological characteristics of electrospun membranes of P(VdF-HFP) under different processing parameters

Sample ref. (as in Fig. 1)	Polymer concentration (wt.%)	Acetone:DMAc (w/w)	Applied voltage (kV)	Fiber diameter range (μm)	AFD (μm)
A	12	7/3	18	0.1–1.2	0.6
B	14	7/3	18	0.3–3.0	0.8
C	16	7/3	18	0.6–1.4	1.0
D	18	7/3	18	0.5–3.1	1.5
E	16	7/3	11	0.1–1.8	1.1
F	16	7/3	24	0.4–3.8	1.5
G	16	5/5	18	0.3–1.5	0.9
H	16	3/7	18	0.3–1.5	1.0

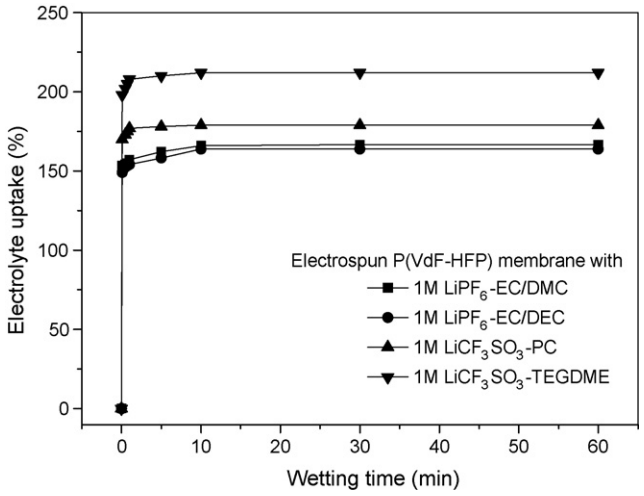

Fig. 2. Electrolyte uptake (ε, %) of electrospun P(VdF-HFP) membrane with different liquid electrolytes.

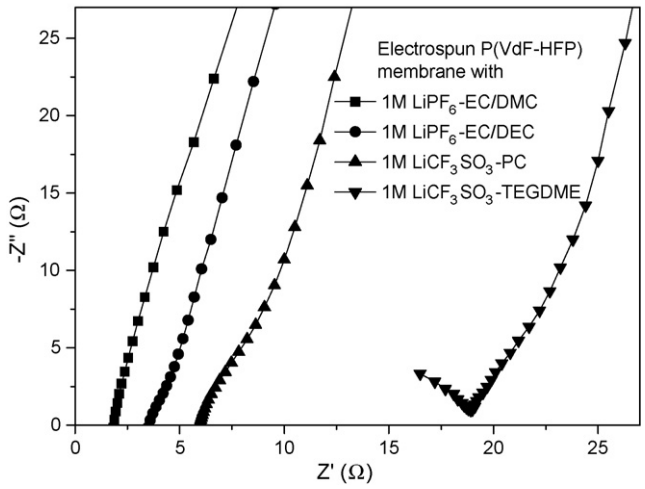

Fig. 3. AC impedance spectra at 20 °C of PEs based on electrospun P(VdF-HFP) membrane.

1 M $LiPF_6$ in EC/DMC/diethyl carbonate (DEC) (1:1:1, v/v/v) has been reported for electrospun membranes of P(VdF-HFP) with AFD ∼1 μm [17]. The electrolyte uptake of the fibrous membrane in the present study is comparatively lower, a direct consequence of the lower porosity achieved. Nevertheless, the membrane has good wettability by the electrolytes and a higher electrolyte uptake compared with that reported for the Celgard polyolefin separator (uptake ∼130%, porosity ∼40%) [13]. The electrospun membrane exhibits sufficient mechanical strength and self-standing properties even after being activated with the liquid electrolytes.

3.3. AC impedance and ionic conductivity

The ionic conductivities of the PEs were measured at different temperatures by the AC impedance method. The impedance responses are typical of electrolytes where the bulk resistance is the major contribution towards the total resistance. An inclined straight line towards the real axis representing the electrode|electrolyte double layer capacitance behaviour is observed over the whole range of frequency evaluated. This indicates that there is only a minimal contribution from grain boundary resistance to the total resistance. Typical AC impedance spectra obtained at 20 °C for the PEs are shown in Fig. 3. Only the PE based on $LiCF_3SO_3$ in TEGDME shows an arc portion in the spectra, which represents a minor contribution from the grain boundaries to the total resistance. The real-axis intercept of the straight line represents the bulk resistance of the given electrolyte (R_b). At 20 °C, R_b varies between 2 and 19 Ω for the PEs. The R_b of $LiCF_3SO_3$ in TEGDME is higher than that of the other systems indicating a lower ionic conductivity for this PE. With increase in temperature, R_b is progressively reduced, revealing a corresponding enhancement in ionic conductivity.

Variation of the ionic conductivities of the PEs with temperature is shown in Fig. 4. The PEs under study comprise a solid polymer fibre phase, a partially swollen amorphous fibre phase and a liquid electrolyte phase encapsulated in the pores of the membrane [6,13,14]. Two ion conduction paths have been postulated for porous membrane-based PEs: one is a high conduction path through the liquid electrolyte phase and the other is a slow conduction path through the swollen polymer phase [6,17]. Studies reported by Saunier et al. [6] on the conductivities of gel electrolytes based on PVdF show that the contribution to the conductivity by the PVdF structure swollen with electrolyte may be neglected with respect to that of the porous volume filled with electrolyte. Hence, the overall ionic conductivity of the PE is highly influenced by the liquid electrolyte phase. A linear relationship between ionic conductivity and temperature is observed for all the PEs examined here. The variation of conductivity with temperature is minimal for PEs with higher conductivity, namely $LiPF_6$ in EC/DMC and EC/DEC. For these systems, the ionic conductivities at 20 °C are 4.7×10^{-3} and 2.5×10^{-3} S cm^{-1},

Table 2
Physical properties of organic solvents in electrolytes

Properties	EC[a]	DMC[a]	DEC[a]	PC[a]	TEGDME[b]
Molecular weight	88	90	118	102	222
Normal melting point (°C)	36.4	4.6	−74.3	−48.8	−30
Viscosity at 25 °C (cP)	1.90 (40)	0.59 (20)	0.75	2.53	4.05
Density at 25 °C (g cm^{-3})	1.321	1.063	0.969	1.200	1.009
Dielectric constant at 25 °C	89.78	3.107	2.805	64.92	7.9

Superscript values refer to temperature at which property is measured.
[a] Ref. [20].
[b] Aldrich catalogue for Product No. 24,116-4.

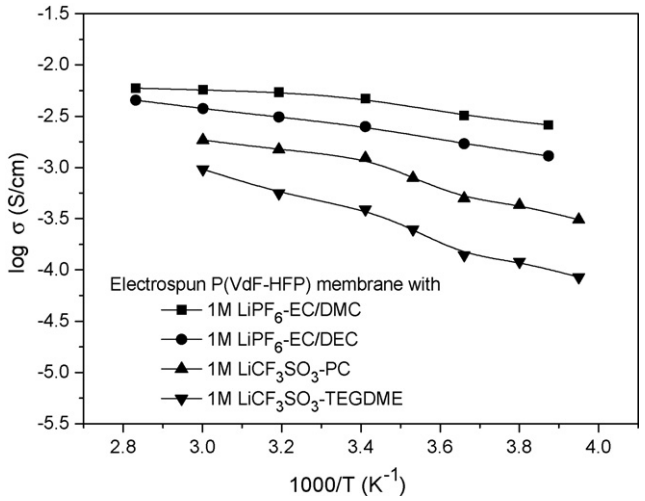

Fig. 4. Variation of ionic conductivity with temperature of PEs based on electrospun P(VdF-HFP) membrane.

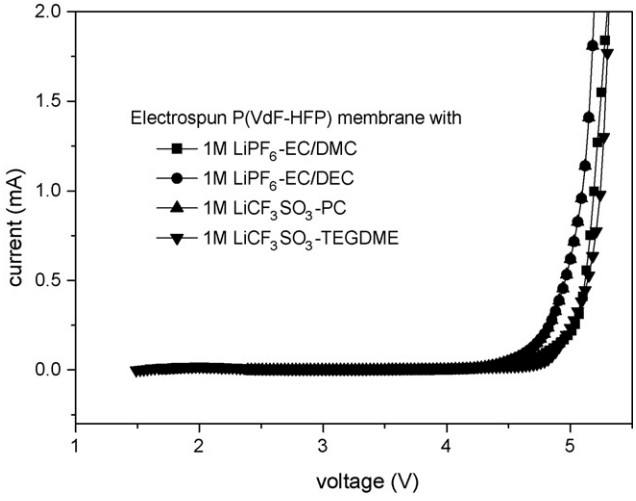

Fig. 5. Electrochemical stability by linear sweep voltammetry of PEs based on electrospun P(VdF-HFP) membrane.

respectively. The higher ionic conductivity is a result of the lower viscosities of the alkyl ether solvents DEC and DMC at room temperature and the high dielectric constant of the constituent EC in the solvent mixture, which is helpful by causing a high dissociation of the lithium salt.

Lithium-salt electrolytes with a mixture of the cyclic carbonate EC and linear carbonates DMC or DEC are known to provide favourable properties to lithium batteries, which include high ionic conductivity [20]. One molar $LiPF_6$ in EC/DMC is reported to have an ionic conductivity of 10.7×10^{-3} S cm^{-1} at 25 °C [22]. The extent of conductivity loss for this electrolyte due to the presence of the electrospun membrane in the PE is thus seen to be very low (i.e., a loss factor of <0.5, compared with the conductivity of 4.7×10^{-3} S cm^{-1} for the PE at 20 °C). Using a microporous PVdF membrane prepared by phase inversion as the host matrix for PEs with 1 M $LiPF_6$ in mixed carbonates as electrolyte solvents, a conductivity loss factor of ~3 has been reported [6].

In summary, it is found that the fully interconnected pore structure of the electrospun membrane used in the present study allows easier passage of ions between the electrodes. The lower conductivity for PE based on TEGDME solvent could be due to its lower dielectric constant affecting the dissociation of lithium salt, and to the higher viscosity limiting the mobility of ions in the electrolyte. Nevertheless, this PE has a conductivity of 0.4×10^{-3} S cm^{-1} at 20 °C, which is considered to be sufficient for practical applications in lithium batteries.

3.4. Electrochemical properties

The electrochemical stability window of the electrospun P(VdF-HFP)-based PEs is shown in Fig. 5. The order of electrochemical stability is: 1 M $LiCF_3SO_3$ in TEGDME (4.9 V) > 1 M $LiPF_6$ in EC/DMC (4.8 V) > 1 M $LiCF_3SO_3$ in PC = 1 M $LiPF_6$ in EC/DEC (4.6 V). Thus, the PEs have good anodic stability, above 4.5 V versus Li/Li$^+$, i.e., sufficient to be compatible with most of the common materials used for lithium battery cathodes. Earlier studies also have reported high electrochemical stability for PEs based on electrospun PVdF [13,14], P(VdF-HFP) [17] and PAN [18]. Although ionic conduction is occurring mainly through the entrapped liquid electrolyte in the porous structure, the partially swollen fibrous matrix with large surface area contributes significantly in enhancing the electrochemical stability of the PE [13,14].

Compatibility of the electrolyte with the lithium metal anode is an important factor that determines the cycle performance of the lithium cells. The impedance behaviour of PEs based on an electrospun P(VdF-HFP) membrane with 1 M $LiPF_6$ in EC/DMC and EC/DEC on lithium metal is presented in Fig. 6. The impedance characteristics at an initial stage and after storage for 7 days are shown. Impedance spectra in the form of semicircles typical of electrolytes with contributions from bulk electrolyte resistance (R_b) and electrode|electrolyte interfacial resistance (R_f) are observed. The real axis intercept at the high frequency end of the spectrum denotes R_b of the electrolyte and is very low (between 5.6 and 6.5 Ω). These values agree well with the low R_b observed for these electrolytes in SS/PE/SS cells

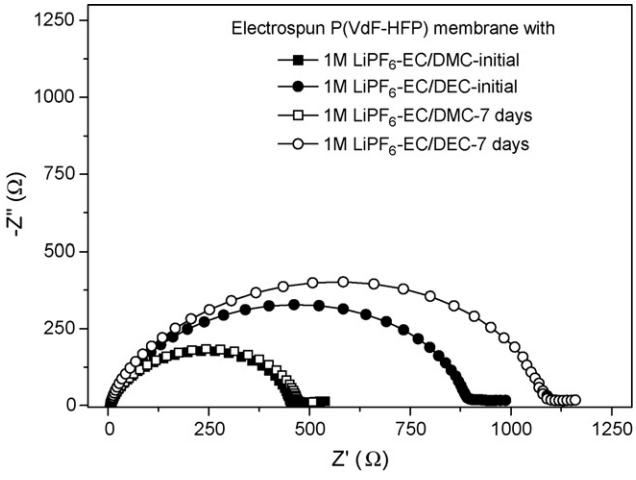

Fig. 6. Impedance behaviour of Li/PE/Li cells initially and after 7 days storage. PEs based on electrospun P(VdF-HFP) membrane with 1M $LiPF_6$ in EC/DMC and EC/DEC.

(2–3.5 Ω, detailed above in Section 3.3). There is no appreciable increase in R_b with storage for 7 days. A similar observation of a constant R_b with storage has been observed in the earlier studies with PEs based on electrospun fibrous membranes of PVdF [13,14]. This behaviour is indicative of a good retention of the ionic conductivity of the PE consisting of a swollen fibrous structure. By contrast, the solvent composition has an appreciable influence on the R_f of the electrolyte on lithium metal. The initial R_f value for an electrolyte with EC/DMC is nearly half of that for EC/DEC (458 and 904 Ω, respectively) and with storage for 7 days, R_f increases to 475 Ω (i.e., by ∼4%) for the EC/DMC system, and to 1130 Ω (i.e., by ∼25%) for the EC/DEC system. The increase in R_f with time is the result of the formation of a passive layer caused by a reaction between the aprotic solvents and lithium electrodes during storage [23]. The superior compatibility of the electrolyte based on EC/DMC compared with EC/DEC could be the effect of the lower viscosity of DMC with respect to DEC. Electrolytes of low viscosity can provide better wetting over the electrode and facilitate easier penetration of ions.

3.5. Evaluation in Li/LiFePO$_4$ cell

Based on its high ionic conductivity and better compatibility with a lithium anode, a PE comprised of electrospun P(VdF-HFP) with 1 M $LiPF_6$ and EC/DMC was selected for evaluation in a lithium metal battery with a $LiFePO_4$ cathode at room temperature. $LiFePO_4$ has attracted much attention as the next-generation cathode material. It has a high theoretical capacity of 170 mAh g^{-1}, an operating potential of 3.4 V, and excellent cycling properties [21,24,25]. Compared with the transition metal oxides presently used as cathode materials in lithium-ion batteries, $LiFePO_4$ is non-toxic, cheaper and easy to prepare. The initial discharge capacity at current densities of 0.1 and 1 C of a Li/$LiFePO_4$ cell with electrospun P(VdF-HFP) based PE is presented in Fig. 7. Relatively high cathode utilizations corresponding to 83.5 and 73.5% of theoretical capacity are achieved

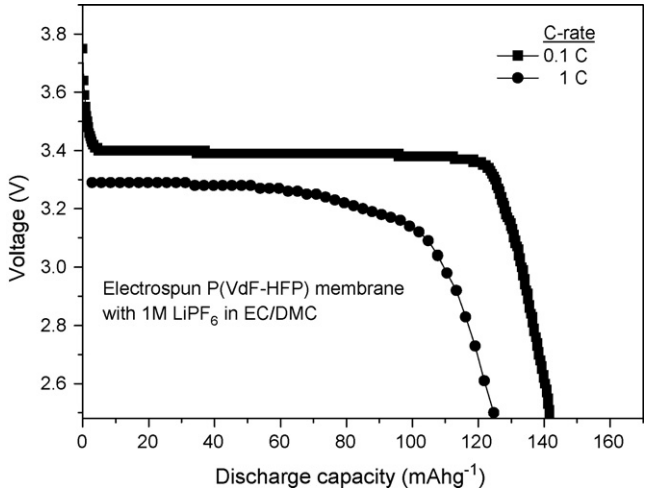

Fig. 7. Initial discharge capacity of Li/$LiFePO_4$ cell using PE based on electrospun P(VdF-HFP) membrane with 1 M $LiPF_6$ in EC/DMC at 0.1 and 1.0 C rates (2.5–4.0 V; room temperature).

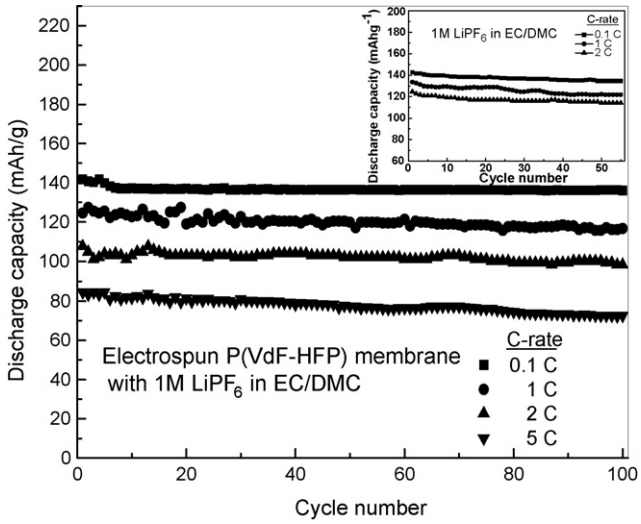

Fig. 8. Cycle performance of Li/$LiFePO_4$ cell using PE based on electrospun P(VdF-HFP) membrane with 1 M $LiPF_6$ in EC/DMC at different C rates. (Inset) Cycle performance of Li/$LiFePO_4$ cell using liquid electrolyte 1 M $LiPF_6$ in EC/DMC (2.5–4.0 V; room temperature).

at the 0.1 and 1 C-rates, respectively. The decrease in discharge capacity at the higher C-rate is usually observed for $LiFePO_4$-based cells and is attributed to the slow diffusion of lithium ions across the solid two-phase boundary of $LiFePO_4$ and $FePO_4$ [24].

The cycle performance of the cell up to 100 cycles and at different C-rates is shown in Fig. 8. The initial discharge capacities at the 0.1, 1, 2 and 5 C-rate are 142, 125, 108 and 85 mAh g^{-1}, respectively. After 100 cycles, the corresponding capacities are 136, 117, 98 and 72 mAh g^{-1}. Thus, capacity fading per cycle is low, namely between 0.04 and 0.15% at the applied C-rates. The remarkably good cycle properties of the cells, even at high current densities, demonstrate the suitability of the electrospun membrane based PE for this cell. In an earlier study [21] an evaluation was made of the performance of Li/$LiFePO_4$ cells under similar conditions using a liquid electrolyte of 1 M $LiPF_6$ in EC/DMC. The cycle properties of that cell at the 0.1, 1 and 2 C-rate are shown in the inset of Fig. 8. The initial discharge capacities are 143, 134 and 125 mAh g^{-1} at the 0.1, 1 and 2 C-rate, respectively. Thus, it is seen that the performance of PE is as good as the liquid electrolyte at the lowest current density of 0.1 C. At the 1 and 2 C rates, the discharge capacities provided by the PE are marginally lower than those obtained with the liquid electrolyte. This probably results from the lower ionic conductivity and hence slower reaction kinetics of the PE. The capacity fading per cycle at all the C-rates is comparable for both the PE and liquid electrolyte. This evaluation demonstrates the suitability of PE based on an electrospun membrane for lithium metal battery applications.

4. Conclusions

P(VdF-HFP) fibrous membranes have been prepared by electrospinning of the polymer solution in a mixed solvent of acetone and DMAc. The effect of spinning process parameters such

as polymer concentration, applied voltage and solvent ratio on the AFD and morphology of the membrane has been evaluated. Polymer concentration has the largest effect, followed by applied voltage and solvent ratio. A fibrous membrane with uniform morphology and an AFD of 1 μm has been prepared under the optimized conditions of 16 wt.% solution in acetone:DMAc (7:3, w/w) at 18 kV. The PEs are prepared by activating the membrane with different liquid electrolytes. High ionic conductivities in the range of 10^{-3} S cm^{-1} at 20 °C are exhibited by the PEs. This performance is attributed to the easy passage of the liquid electrolyte through the fully interconnected pore structure of the membrane. The PEs have good electrochemical stability at >4.5 V versus Li/Li$^+$, and a reasonably stable R_f on lithium metal. A PE based on electrospun P(VdF-HFP) with 1 M $LiPF_6$ in EC/DMC has been evaluated in a lithium metal battery with a $LiFePO_4$ cathode for discharge capacity and cycle performance at different C-rates. The resulting good performance indicates that PEs based on electrospun P(VdF-HFP) membranes are suitable for application in high-performance lithium metal batteries.

Acknowledgements

This research has been supported by the Ministry of Information and Communication (MIC), Korea, under the Information Technology Research Center (ITRC) support program that is supervised by the Institute of Information Technology Assessment (IITA). Gouri Cheruvally is grateful to KOFST for the award of a Brain Pool Fellowship, and Jae-Won Choi and Jae-Kwang Kim acknowledge partial support by the Post Brain Korea 21 Project in 2006.

References

[1] J.M. Tarascon, A.S. Gozdz, C. Schmutz, F. Shokoohi, P.C. Warren, Solid State Ionics 86–88 (1996) 49.
[2] A. Subramania, N.T. Kalyanasundaram, G. Vijayakumar, J. Power Sources 153 (2006) 177.
[3] Z. Jiang, B. Carroll, K.M. Abraham, Electrochim. Acta 42 (1997) 2667.
[4] Z. Wang, Z. Tang, Mater. Chem. Phys. 82 (2003) 16.
[5] J.W. Choi, J.H. Kim, G. Cheruvally, J.H. Ahn, K.W. Kim, H.J. Ahn, J.U. Kim, J. Ind. Eng. Chem. 12 (2006) 939.
[6] J. Saunier, F. Alloin, J.Y. Sanchez, G. Caillon, J. Power Sources 119–121 (2003) 454.
[7] W. Pu, X. He, L. Wang, C. Jiang, C. Wan, J. Membr. Sci. 272 (2006) 11.
[8] J.W. Choi, J.K. Kim, G. Cheruvally, J.H. Ahn, H.J. Ahn, K.W. Kim, Electrochim. Acta 52 (2007) 2075.
[9] H. Wang, H. Huang, S.L. Wunder, J. Electrochem. Soc. 147 (2000) 2853.
[10] J. Doshi, D.H. Reneker, J. Electrostat. 35 (1995) 151.
[11] Z.M. Huang, Y.Z. Zhang, M. Kotaki, S. Ramakrishna, Compos. Sci. Technol. 63 (2003) 2223.
[12] D. Li, Y. Xia, Adv. Mater. 16 (2004) 1151.
[13] S.W. Choi, S.M. Jo, W.S. Lee, Y.R. Kim, Adv. Mater. 15 (2003) 2027.
[14] J.R. Kim, S.W. Choi, S.M. Jo, W.S. Lee, B.C. Kim, Electrochim. Acta 50 (2004) 69.
[15] S.S. Choi, Y.S. Lee, C.W. Joo, S.G. Lee, J.K. Park, K.S. Han, Electrochim. Acta 50 (2004) 339.
[16] S.W. Lee, S.W. Choi, S.M. Jo, B.D. Chin, D.Y. Kim, K.Y. Lee, J. Power Sources 163 (2006) 410.
[17] J.R. Kim, S.W. Choi, S.M. Jo, W.S. Lee, B.C. Kim, J. Electrochem. Soc. 152 (2005) A295.
[18] S.W. Choi, J.R. Kim, S.M. Jo, W.S. Lee, Y.R. Kim, J. Electrochem. Soc. 152 (2005) A989.
[19] K.S. Yun, B.Y. Cho, S.M. Jo, W.S. Lee, W.I. Cho, K.U. Park, WO 01/89020 A1 to 01/89023 A1, Korea Institute of Science and Technology, 2001.
[20] K. Xu, Chem. Rev. 104 (2004) 4303.
[21] J.K. Kim, J.W. Choi, G. Cheruvally, J.U. Kim, J.H. Ahn, G.B. Cho, K.W. Kim, H.J. Ahn, J. Power Sources 166 (2007) 211.
[22] M. Schmidt, U. Heider, A. Kuehner, R. Oesten, M. Jungnitz, N. Iganat'ev, P. Sartori, J. Power Sources 97/98 (2001) 557.
[23] H. Sung, Y. Wang, C. Wan, J. Electrochem. Soc. 145 (1998) 1207.
[24] A.K. Padhi, K.S. Nanjundaswamy, J.B. Goodenough, J. Electrochem. Soc. 144 (1997) 1188.
[25] K. Striebel, J. Shim, A. Sierra, H. Yang, X. Song, R. Kostecki, K. McCarthy, J. Power Sources 146 (2005) 33.